Development of Actionable Targets of Multi-kinase Inhibitors (AToMI) screening platform to dissect kinase targets of staurosporines in glioblastoma cells

Authors: Oxana V. Denisova[1], Joni Merisaari[1,2], Amanpreet Kaur[1], Laxman Yetukuri[1,3], Mikael Jumppanen[1], Carina von Schantz-Fant[3], Michael Ohlmeyer[4,5], Krister Wennerberg[3,6], Tero Aittokallio[3,7,8], Mikko Taipale[9], Jukka Westermarck[1,2]*

Affiliations:

[1]Turku Bioscience Centre, University of Turku and Åbo Akademi University, Turku, Finland.

[2]Institute of Biomedicine, University of Turku, Turku, Finland.

[3]Institute for Molecular Medicine Finland, HiLIFE, University of Helsinki, Helsinki, Finland.

[4]Icahn School of Medicine at the Mount Sinai, NY, USA.

[5]Atux Iskay LLC, Plainsboro, NJ, USA.

[6]Biotech Research & Innovation Centre, University of Copenhagen, Copenhagen, Denmark.

[7]Centre for Biostatistics and Epidemiology, University of Oslo, Oslo, Norway.

[8]Institute for Cancer Research, Oslo University Hospital, Oslo, Norway.

[9]Donnelly Centre, University of Toronto, Toronto, Canada.

*Corresponding author. Email: jukwes@utu.fi

ABSTRACT

Therapeutic resistance to kinase inhibitors constitutes a major unresolved clinical challenge in cancer and especially in glioblastoma. Multi-kinase inhibitors may be used for simultaneous targeting of multiple target kinase and thereby potentially overcome kinase inhibitor resistance. However, in most cases identification of the target kinases mediating therapeutic effects of multi-kinase inhibitors has been challenging. To tackle this important problem, we developed an Actionable Targets of Multi-kinase Inhibitors (AToMI) strategy and used it for characterization of glioblastoma target kinases of staurosporine derivatives displaying synergy with protein phosphatase 2A (PP2A) reactivation. AToMI consists of interchangeable modules combining drug-kinase interaction assay, siRNA high-throughput screening, bioinformatics analysis and validation screening with more selective target kinase inhibitors. As a result, AToMI analysis revealed AKT and mitochondrial pyruvate dehydrogenase kinase PDK1 and PDK4 as kinase targets of staurosporine derivatives UCN-01, CEP-701, and K252a that synergized with PP2A activation across heterogeneous glioblastoma cells. Based on these proof-of-principle results we propose that application and further development of AToMI for clinically applicable multi-kinase inhibitors could provide significant benefits in overcoming the challenge of lack of knowledge of target specificity of multi-kinase inhibitors.

INTRODUCTION

Multi-kinase inhibitors (MKIs) and more targeted kinase inhibitors are often used in cancer therapies without exact knowledge of the kinases targeted for the therapeutic benefit (Klaeger *et al*, 2017; Lin *et al*, 2019; Montoya *et al*, 2021; Tang *et al*, 2018). Staurosporines (STSs) are a large family of MKIs originally derived from bacterial alkaloid staurosporine (Gani & Engh, 2010). STSs function as classical ATP mimics and are known to inhibit up to 50 kinases with approximately similar efficiency (Gani & Engh, 2010; Klaeger *et al.*, 2017; Tang *et al.*, 2018). Regardless of their very wide target spectrum and reputation as "dirty kinase inhibitor" several STS derivatives have reached or has been tested in the clinics. Midostaurin (PKC412) is approved for the treatment of FLT3-mutated acute myeloid leukemia (Montoya *et al.*, 2021), whereas another STS derivative UCN-01 (7-hydroxystaurosporine) was tested in phase II clinical trials in metastatic melanoma and relapsed T-Cell Lymphomas (NCT00082017). However, in most cases it is not well established what are the actual kinase inhibitor targets the inhibition of which mediates the therapeutic effects in different indications. Further, in a case of brain tumors STS derivatives are compromised by their pharmacokinetic properties as they do not cross the brain-blood barrier (BBB).

Development of MKIs towards clinical use would benefit from a better understanding of the kinase targets mediating both the therapeutic and potential toxic effects in each disease application. However, generalizable strategies for analysis of actionable MKI targets are currently missing. Here, we present Actionable Targets of Multi-kinase Inhibitors (AToMI) as a generalizable approach to identify actionable co-targets of MKIs. We propose that application of AToMI for clinically applicable MKIs would provide significant benefits in overcoming the challenge of lack of knowledge of target specificity of kinase inhibitors.

63 **RESULTS**

64

65 **Strategy for characterization of Actionable Targets of Multi-kinase Inhibitors (AToMI)**

66 Protein phosphatase 2A (PP2A) inhibition drives resistance to several kinase inhibitors in
67 multiple cancer types and thereby PP2A reactivation could be envisioned as a novel therapeutic
68 opportunity to overcome kinase inhibitor resistance (Kauko *et al*, 2020; Kauko *et al*, 2018;
69 Vervoort *et al*, 2021; Westermarck, 2018). Related to glioblastoma (GB), we recently
70 demonstrated strong synergistic activity between PP2A reactivation and clinically tested STS
71 derivative UCN-01 (Kaur *et al*, 2016). However, as UCN-01 targets approximately 50 different
72 kinases at nanomolar concentrations (Gani & Engh, 2010; Klaeger *et al.*, 2017) it remains
73 unclear which one(s) of these kinases are involved in synthetic lethality (SL) phenotype
74 observed in combination with PP2A reactivation. To systematically map the UCN-01 co-target
75 interactions relevant to synergy with PP2A reactivation, we devised a functional screening
76 platform consisting of the following steps (Fig. 1):

77 1) Chaperone interaction assay to compare direct kinase binding between UCN-01 and STS
78 derivatives displaying differential synergism with PP2A reactivation in GB cells.

79 2) siRNA screening for synergistic interaction between PP2A reactivation and targeting of the
80 individual kinase hits from the step 1.

81 3) Bioinformatics analysis of actionable kinase networks based on steps 1 and 2 for
82 identification of selective small molecule inhibitors for the critical kinase nodes in the network.

83 4) Small molecule kinase inhibitor validation experiments.

84

85 As this strategy could be generally suitable for functional filtering of targets of MKIs, we
86 hereby refer to the screening platform as characterization of Actionable Targets of Multi-kinase

87 Inhibitors (AToMI). The individual technologies used in AToMI are interchangeable with the

88 most suitable technologies for any other application AToMI would be used for.

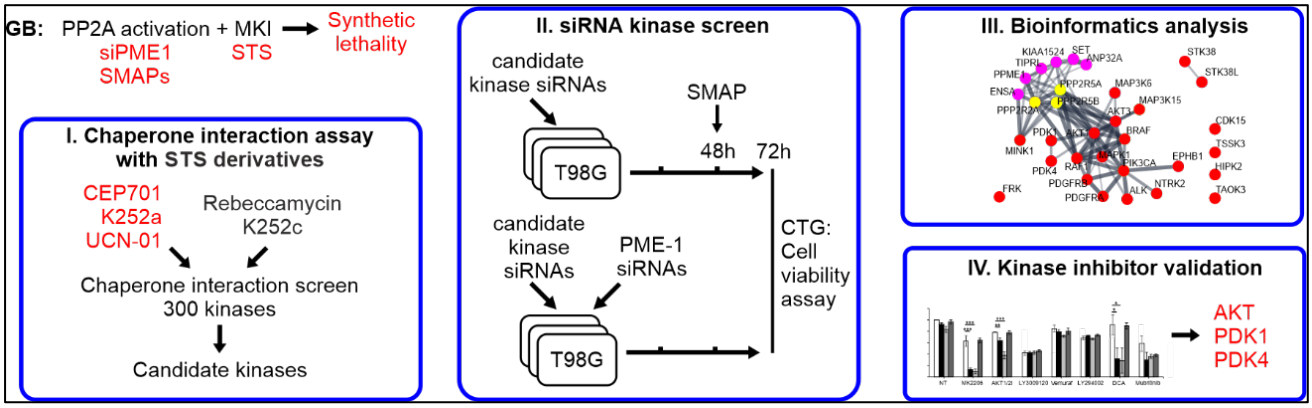

89

90 **Figure 1. A schematic illustration of AToMI screening platform**.

91

92 **Use of AToMI to identify actionable kinase targets of STSs synergizing with PP2A**

93 **reactivation**

94 By using AToMI, we compared the kinase target profiles of STS derivatives UCN-01, CEP-

95 701 and K252a, previously shown to synergize with PP2A reactivation, against STS derivatives

96 K252c and rebeccamycin that did not synergize with PP2A reactivation (Kaur *et al.*, 2016).

97 The differential synergistic activities of these STS derivatives in combination with a small

98 molecule activator of PP2A (SMAPs), NZ-8-061 (Sangodkar *et al*, 2017), were confirmed by

99 colony growth assay in T98G cells (Fig. 2A). In the first step of AToMI, all five STS

100 compounds were screened for their direct kinase protein binding against 300 kinases by

101 Chaperone interaction assay (Taipale, 2018) (Fig. 2B, S1, Table S1). This assay measures the

102 interaction of kinases with their chaperone Cdc37 in the presence (or absence) of kinase

103 inhibitors. Binding of the inhibitor to its target leads to thermodynamic stabilization of the

104 target, which can be detected as weaker interaction between the kinase and Cdc37 (Taipale *et*

105 *al*, 2013). Using log2 -0.5-fold reduction in chaperone binding as a threshold for interaction, a

106 total of 29 candidate kinases were identified to differentially interact with STS derivatives that

synergized with PP2A (CEP-701, K252a, and UCN-01), but not with rebeccamycin or K252c (Table S2).

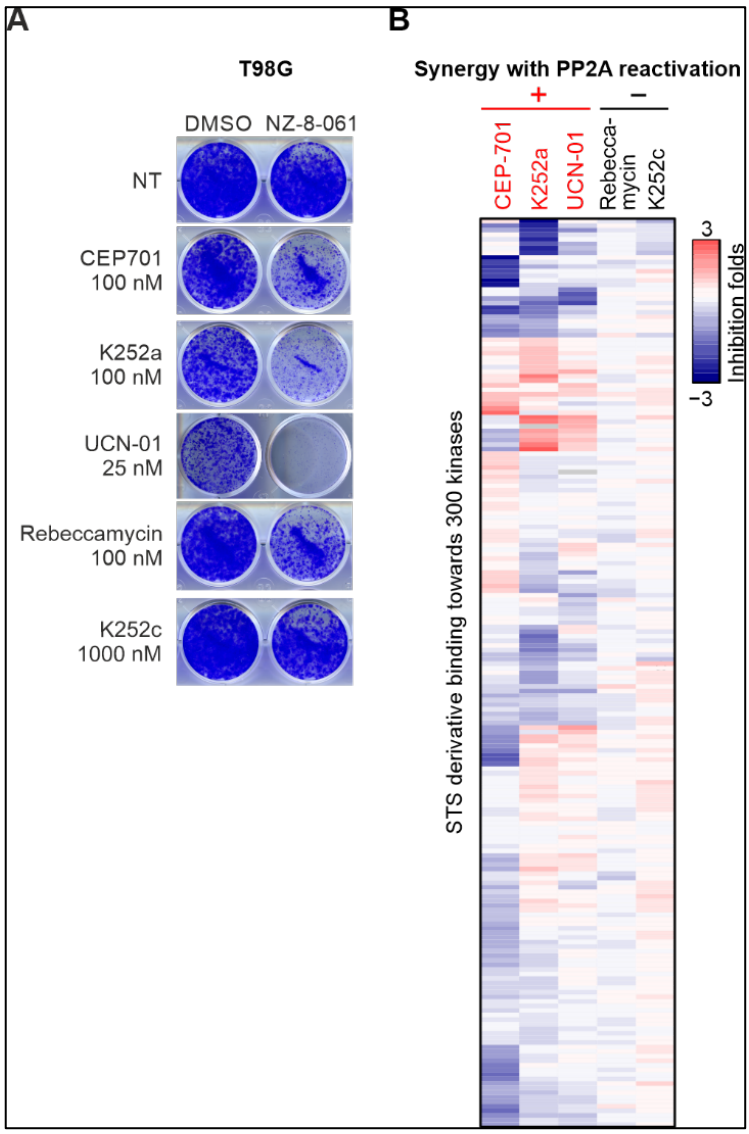

Figure 2. Chaperone interaction assay. A) Representative images of colony formation assay in T98G cells treated vehicle (DMSO) and NZ-8-061 in combination with STS derivatives. **B)** Heat map representation of interaction of STS derivatives, CEP-701, K252a, UCN-01, rebeccamycin and K252c, with 300 protein kinases by Chaperone interaction assay. Color scale bar indicates log2 fold changes of kinase/Cdc37 interactions between inhibitor and DMSO treatments.

In the siRNA screening step of AToMI, the goal was to identify among the shared targets of CEP-701, K252a, and UCN-01, individual kinases whose co-inhibition resulted in synergism with PP2A reactivation in cell viability inhibition. The screen was conducted with a custom human kinase siRNA library, which had three non-overlapping siRNAs targeting each kinase. In addition to 29 candidate kinases from the step 1, the siRNA library was extended to include

121 8 additional kinases frequently altered in GB (Brennan *et al*, 2013; Patel *et al*, 2014) (Table
122 S3). The siRNAs were reverse transfected to T98G cells, and cells were subsequently exposed
123 to PP2A reactivation by NZ-8-061 treatment (Fig. 3A). In the validation screen, we included
124 selected 25 kinases in combination with PME-1 siRNAs to evaluate similarity in drug
125 sensitization between chemical (NZ-8-061) and genetic (PME-1 siRNA) PP2A reactivation
126 (Fig. 3A). The efficacy of PME-1 depletion by tree independent siRNAs was validated by
127 western blotting from parallel samples (Fig. S2). For each kinase siRNA, Gene Activity
128 Ranking Profiles and synergy scores were computed as described in the methods section of
129 siRNA screens. Notably, regardless of the marked differences in the targeting approaches, most
130 of the kinases targeted in both screens were found to synergize both with NZ-8-061 treatment
131 and PME-1 depletion (Fig. 1B), validating both the shared PP2A-induced mode of action, and
132 the broad impact of PP2A activity in kinase inhibitor tolerance in GB.
133
134 STRING protein-protein interaction network analysis of the AToMI candidate kinases from
135 the step 2 revealed enrichment of RTK/RAF/MAPK (PDGFR, RAF1, BRAF and MAPK1) and
136 PI3K/AKT/mTOR pathways (PIKCA, AKT1 and AKT3), as well as mitochondrial pyruvate
137 dehydrogenase kinase (PDK1 and PDK4) among the kinases connected to PP2A B-subunits
138 responsible for SL by STS treatment and PME-1 depletion (Fig. 3C) (Kaur *et al.*, 2016). As
139 each of these kinase modules were represented also among the kinases that were shared
140 between the NZ-8-061 and siPME-1 synergy targets, we proceeded to testing these GB
141 signaling nodes by selective small-molecule inhibitors. Selectivity of the chosen small-
142 molecule inhibitors was evaluated based recently published target selectivity databases, and for
143 some compounds also by Chaperone interaction assay (Table S4) (Klaeger *et al.*, 2017; Tang
144 *et al.*, 2018). To facilitate translation of the results, we also considered oral bioavailability and
145 BBB permeability of the compounds in drug selection. The selected 7 kinase inhibitors were

146 screened for cell viability effects in T98G cells with two SMAPs, NZ-8-061 and DBK-1154
147 (Merisaari *et al*, 2020). As a control, we used an inactive SMAP analog DBK-766, that binds
148 PP2A but is unable to reactivate it even at a concentration of 20 µM *in vitro* (Sangodkar *et al.*,
149 2017). The results show that both NZ-8-061 and DBK-1154 sensitized T98G cells to MK-2206
150 and AKT1/2i (AKT signaling) (Shariati & Meric-Bernstam, 2019), and DCA (PDK inhibitor)
151 (Michelakis *et al*, 2010; Stacpoole, 2017) used at concentrations that engage their aimed target
152 kinase (Fig. 4A, S3A, B). Importantly, the inactive SMAP (DBK-766) did not synergize with
153 any of these kinase inhibitors (Fig. 4A) and another PDK inhibitor, lipoic acid (Stacpoole,
154 2017), recapitulated the synergy with SMAPs (Fig. S3C, D). Further validating PP2A
155 reactivation as the mechanism inducing the synergistic drug interaction, also PME-1 inhibition
156 synergized with both MK-2206 and DCA treatments (Fig. S3E). On the other hand, RAF
157 inhibitors (LY3009120 and Vemurafenib), PI3K inhibitor (LY294002), or MINK1 inhibitor
158 (mubritinib) did not display significant combinatorial effect with PP2A reactivation (Fig. 4A).
159
160 Collectively, these results demonstrate the usefulness of AToMI screening for identification of
161 individual actionable target kinases for MKIs.

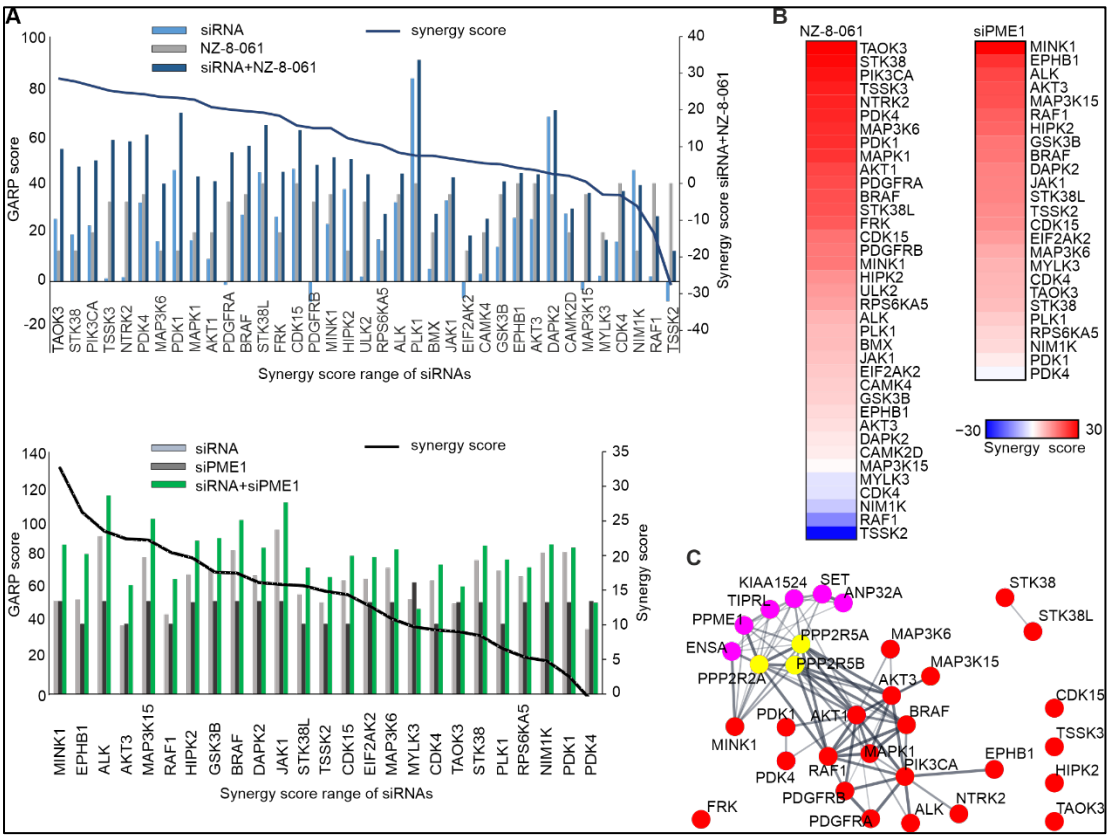

Figure 3. siRNA screening to kinases involved in GB cell synthetic lethality in combination with PP2A reactivation. A) GARP scores of siRNA screen in T98G cells under NZ-8-061-treatment or PME-1 depletion (left axis). Kinases were ordered according to synergy scores (right axis). **B)** Heat map representation of kinases involved in synthetic lethality in NZ-8-061-treated and PME-1-depleted T98G cells. Color bar indicates the synergy scores. **C)** STRING interactive mapping of screen kinase hits onto PP2A network.

Validation of AToMI results in heterogeneous GB cell lines

Cellular heterogeneity and high intrinsic therapy resistance of GS as well as presence of GSCs are major challenges related GB therapies (Gimple *et al*, 2019). We then applied AKT and PDK inhibitors in combination with SMAPs across two additional established GB cell lines, E98 and U87MG, and two patient-derived GSC lines, BT-CD133^{+} and BT12 (Le Joncour *et al*, 2019; Merisaari *et al.*, 2020). However, consistently with high intrinsic kinase inhibitor resistance of GB cells (Merisaari *et al.*, 2020; Mooney *et al*, 2019), none of the kinase inhibitor monotherapies used at doses that effectively inhibited their intended targets (Fig. S3A, B), induced cytotoxic response (i.e. more than 50% reduction in cell viability) (Fig. 4B). Further, illustrative of the challenge with heterogeneity of GB cell therapy responses, maximal inhibition of cell viability with any doublet combinations was highly variable across the cell

180 lines. In example, BT-CD133^{+} cells were fully resistant to combination of AKT inhibition and
181 PP2A reactivation, whereas the maximal effect of DCA and SMAP combination on E98 cell
182 viability was only 50%. However, indicative of GB cell selectivity of the drug interactions, the
183 human fibroblasts did not show any signs of synergy between kinase inhibition and SMAPs
184 (Fig. 4B). Additionally, the results were confirmed by colony growth assay (Fig. 4C).

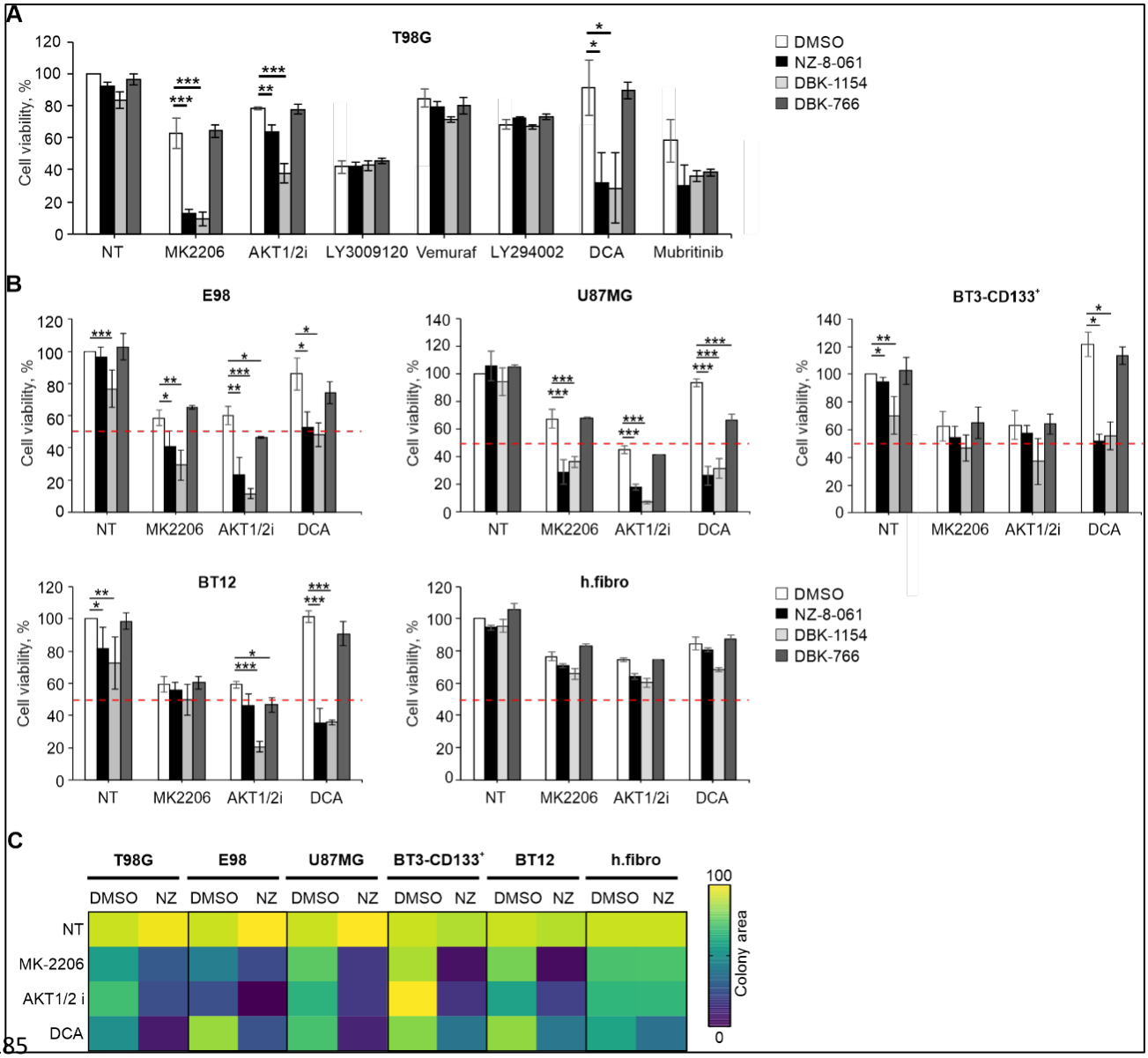

185
186 **Figure 4. Validation of AToMI results in heterogeneous GB cell lines. A-B)** Viability of T98G (A) and
187 established GB, E98 and U87MG, and patient-derived GSCs, BT3-CD133^{+} and BT12, cell lines (B) treated with
188 the selected kinase inhibitors alone or in combination with 8 µM NZ-8-061, 6 µM DBK-1154 or 10 µM DBK-
189 766 for 72 h. Human fibroblasts used as a control of normal cells. Data as mean ±SD (n=3 independent
190 experiments). *P<0.05, **P<0.01, ***P<0.001 by Student's *t*-test. Red striped line indicates 50% inhibition of
191 cell viability which is considered as a cytostatic but not cytotoxic response. **C)** Heat map representation of
192 quantified colony growth assay data in the indicated established GB cell lines, patient-derived GSCs under vehicle

193 (DMSO) or 8 μM NZ-8-061 (NZ) treatment either alone or in combination with indicated kinase inhibitors.
194 Human fibroblasts used as a control of normal cells. (n=2 independent experiments).

195 **DISCUSSION**

196

197 MKIs provide an attractive approach to simultaneously inhibit several oncogenic kinases, and
198 some MKIs (e.g., Sunitinib, PKC412), are clinically used as cancer therapies (Montoya *et al.*,
199 2021). However, similar to more selective kinase inhibitors, all tested MKIs have thus far failed
200 in GB clinical trials (Cruz Da Silva *et al*, 2021). STS derivatives targeting more than 50 kinases
201 (Gani & Engh, 2010) could provide a wide enough polypharmacological kinase inhibitor
202 spectrum to target GB driver mechanisms, even in the case of heterogeneous GB cell
203 populations. However, use of STSs as GB therapeutics is compromised by their inability to
204 cross the BBB. To overcome these limitations, and to better understand GB relevant STS target
205 kinases, we developed the AToMI screening platform. As a result of chaperone interaction
206 assay, we found several kinases which selectively bound to STS derivatives. Then by candidate
207 kinases siRNA screens, we identify kinases that synergized with PP2A reactivation by either
208 PME-1 inhibition or by SMAPs. Notably, the kinases which synergized with PP2A reactivation
209 represent the commonly hyper activated pathways in GB. For example, AKT pathway is one
210 of the most dysregulated pathways in GB, and it was well presented in the siRNA screen as
211 depletion of AKT1, AKT3 and PIK3CA all synergized with PP2A reactivation. Another
212 strongly GB associated signaling mechanism was mitochondrial glycolysis, as depletion of
213 both PDK1 and PDK4 synergized with PP2A reactivation. However, AKT and PDK1-4
214 targeting monotherapies have failed to demonstrate significant survival effects in clinical trials
215 for GB which is consistent with our results that using AKT and PDK-14 inhibitors at doses that
216 inhibit their target kinases has very limited effects on heterogeneous GB cell lines (Dunbar *et*
217 *al*, 2014; Kaley *et al*, 2019; Stacpoole, 2017; Wen *et al*, 2019). The AToMI approach could
218 clearly identify STS targets that synergize with PP2A reactivation in inhibiting viability of
219 heterogenous GB cells. However, as an additional evidence for high degree of resistance of GB

220 cells towards phosphorylation targeting therapies, even the combinations of PP2A reactivation
221 with either AKT or PDK1-4 inhibitors failed to suppress the viability of most GB cells more
222 than 50% which is yet considered only as a cytostatic effect. Therefore, further studies are
223 needed to explore therapeutic impact of the AToMI identified potential combinatorial
224 approaches in faithful brain cancer models. For this purpose, the AToMI approach was also
225 able to identify more selective and BBB permeable kinase inhibitors with similar biological
226 activity than STS.
227
228 Collectively, these results validate the usefulness of AToMI approach for future studies aiming
229 to characterize actionable targets of MKIs in different indications. As the individual
230 technologies used in AToMI are interchangeable with other screening technologies we
231 postulate that AToMI will be widely useful for addressing different biological questions.
232

233 **MATERIALS AND METHODS**

234

235 **Cell culture and reagents**

236 Established human GB cell lines U87MG (gift from Ari Hinkkanen, University of Eastern
237 Finland, Joensuu, Finland), E98-FM-Cherry (gift from William Leenders, Radboud Institute
238 for Molecular Life Sciences, Nijmegen, The Netherlands) and human fibroblasts (gift from
239 Johanna Ivaska, Turku Bioscience, Turku, Finland) were cultured in DMEM (Sigma-Aldrich).
240 T98G cells (VTT Technical Research Centre, Turku, Finland) were cultured in Eagle MEM
241 (Sigma-Aldrich). All growth mediums were supplemented with 10% (except fibroblasts
242 supplemented with 20%) FBS (Biowest), 2 mM L-glutamine and penicillin (50 U/mL)/
243 streptomycin (50 µg/mL). The patient-derived GSCs BT3-CD133^{+} and BT12 (gift from Pirjo
244 Laakkonen and from Kuopio University Hospital, Kuopio, Finland) were cultured as spheroids
245 in DMEM/F12 (Gibco) and supplemented with 2 mM L-glutamine, 2% B27-supplement
246 (Gibco), penicillin (50 U/mL)/ streptomycin (50 µg/mL), 0.01 µg/mL hFGF-β (Peprotech),
247 0.02 µg/mL hEGF (Peprotech) and 15 mM HEPES-buffer (Gibco). All cell cultures were
248 maintained in a humified atmosphere of 5% CO_2 at 37°C.

249

250 The following chemicals were purchased from indicated distributors: AKT1/2 inhibitor, CEP-
251 701, sodium salt of dichloroacetate (DCA), lipoic acid, mubritinib, PKC412 and UCN-01 from
252 Sigma-Aldrich; LY3009120 and vemurafenib from SelleckChem; K252a and rebeccamycin
253 from Enzo Life Sciences; K252c from Tocris Bioscience; LY294002 from Calbiochem; MK-
254 2206 from MedChemExpress. Compounds were dissolved in DMSO or mQ (for DCA) and
255 stored at -20°C. SMAPs (NZ-8-061, DBK-794, DBK-1154 and DBK-766) were kindly
256 supplied by Prof. Michael Ohlmeyer (Atux Iskay LLC, Plainsboro, NJ, USA), were dissolved
257 in DMSO and stored at room temperature protected from light.

258 **Generation of PME-1 knockout T98G cells**

259 *PPME1* deficient T98G cells were generated by CRISPR/Cas9 technology. T98G cells (4 x 10^4
260 cells) were plated into 24-well plate and transduced with lentivirus particles containing
261 lentiCas9-Blast plasmid (Addgene #52962). After 18 hours the media were exchanged with
262 fresh media with blasticidin. A single cell-derived clone of T98G/Cas9 was developed, and
263 further transduced with lentivirus particles containing pKLV-PB-U6gPPME1(BbsI)-
264 PGKpuro2ABFP plasmid (gRNA *PPME-1* exon 14: 5'-ACTTTTCGAGTCTAC
265 AAGAGTGG, ID 183157785, FuGU, Helsinki, Finland). After 18 hours the media were
266 exchanged with fresh media and 48 hours later the media were complemented with puromycin.
267 Cas9-expression and PME-1 knockout efficiency were evaluated by immunoblot analysis.

268

269 **Cell viability assay**

270 Optimized numbers of cells (2.5 x 10^3 to 5 x 10^3) were plated onto 96-well plates and allowed
271 to adhere. After 24 hours, cells were treated with vehicle (DMSO) or the indicated compounds.
272 After 72 hours, cell viability was measured using CellTiter-Glo assay (Promega) according to
273 the manufacturer's instructions using a BioTek Synergy H1 plate reader (BioTek).

274

275 **Colony formation assay**

276 Optimized numbers of cells (3 x 10^3 to 10 x 10^3) were seeded in 12-well plates and allowed to
277 adhere. The patient-derived GSCs were cultured on Matrigel (Becton Dickinson) coated plates.
278 After 24 h, cells were treated with vehicle (DMSO) or the indicated compounds. After 72 hours,
279 drug-containing media were replaced with non-drug containing medium and incubated until
280 the control wells were confluent. Cells were fixed with ice cold methanol and stained with 0.2%
281 crystal violet solution in 10% ethanol. Plates were scanned and colonies were quantified by
282 ImageJ using Colony area plugin (Guzman *et al*, 2014).

283 **Chaperone interaction assay**

284 LUMIER (LUminescence-based Mammalian IntERactome) with BACON (bait control) assay
285 was performed as previously described (Taipale *et al.*, 2013). In short, 3xFLAG-tagged bait
286 proteins are transfected into 293T cells expressing the Chaperone-Renilla (prey) luciferase in
287 a 96-well plate. After two days, cells are treated with kinase inhibitors (or DMSO) for 1 hour
288 before cell lysis. The cell lysates expressing each bait protein are applied to anti-FLAG coated
289 384-well plates, which captures the bait protein. The amount of luminescence in the well, after
290 washing off nonspecifically binding proteins, indicates the interaction between the bait protein
291 with the prey protein. After the luminescence measurement, the amount of bait protein is
292 measured with ELISA, using a different, polyclonal anti-FLAG antibody conjugated to
293 horseradish peroxidase.

294

295 **siRNA screens**

296 A custom human kinase siRNA library containing three non-overlapping siRNAs targeting
297 each of the 37 kinases was purchased from Qiagen (Table S3). Two independent siRNA screens
298 were done in T98G cells. AllStars negative and AllStars Death (Qiagen) were used as negative
299 and positive controls, respectively. In the first screen, the kinase siRNA library was dispensed
300 in black clear bottom tissue-culture treated 384-well plates (Corning 384) using an Echo
301 acoustic dispenser. The assay plates were used right away or used later in which case they were
302 kept sealed in -20°C until used. For transfection, Opti-MEM medium (Gibco) containing
303 Lipofectamine RNAiMAX (Invitrogen, Thermo Fisher Scientific) was added (5 µL per well)
304 using a Multidrop Combi (Thermo Fisher Scientific) and plates were mixed for 15-30 min at
305 room temperature. After that, T98G (500 cells per well) were added in 20 µL of culture medium
306 using the Multidrop Combi. Final siRNA concentration was 12 nM. After transfection, cells
307 were incubated at 37°C for next 48 hours in the presence of 5% CO_2. Then cells were treated

308 with NZ-8-061 (5 μM) for the next 24 hours and cell proliferation was measured by CellTiter-
309 Glo (Promega) according to the manufacturer's instructions using a Pherastar FS plate reader
310 (BMG Labtech). In the second screen, kinase siRNA library in combination with the control
311 (scrambled and AllStars negative) and PME-1 siRNA (three variants, Table S5) was dispensed
312 first as previously described. Then T98G cell were seeded and incubated at 37°C for next 72
313 hours in the presence of 5% CO_2. Cell proliferation was measured by CellTiter-Glo. Using
314 collected data for each plate, the following calculations were performed to obtain percentage
315 inhibition values for all wells (% inhibition=100*((averageneg–averagesample)/(averageneg–
316 averagepos))). From the siRNAs targeting the same kinase, Gene Activity Ranking Profile
317 (GARP) score for the kinase was calculated by taking average of two siRNAs with the highest
318 values in inhibition data (or two lowest siRNA values from viability data) (Marcotte *et al*,
319 2012). Then, the synergy scores for each kinase were computed using Highest Single Agent
320 model (Berenbaum, 1989).
321
322 **Western blotting and antibodies**
323 Cell lysates were prepared and separated by SDS-PAGE as previously described (Merisaari *et*
324 *al.*, 2020). Primary antibodies: PME-1 (Santa Cruz, sc-20086, 1:1000), phospho Akt S473 (Cell
325 Signaling, 9271, 1:1000), phospho PDHE1α S300 (Millipore, ABS194, 1:1000), β-actin
326 (Sigma-Aldrich, A1978, 1:10 000) and GAPDH (HyTest, 5G4cc, 1:10 000). Secondary
327 antibodies were purchased from LI-COR Biotechnology and membranes were scanned using
328 an Odyssey Imager (LI-COR Biotechnology).
329
330 **Bioinformatics analysis**
331 Cytoscape network analysis software (version 3.9.0) (Shannon *et al*, 2003) was used to
332 visualize the STRING interactive map of hit kinases (Szklarczyk *et al*, 2021). For calculation

333 and visualization of synergy scores, dose-response matrix of NZ-8-061 and UCN-01
334 combination data were applied to SynergyFinder (version 2.0) web-application (Ianevski *et al*,
335 2020).
336
337 **Statistical analyses**
338 For cell culture experiments, three biological replicates have been performed, and each
339 condition was tested in triplicate, unless otherwise specified. Data are presented as mean ±SD
340 and statistical analyses were carried out using a two-tailed Student's *t*-test assuming unequal
341 variances. $P<0.05$ was considered statistically significant.
342
343 **Acknowledgements:** We thank the High Throughput Biomedicine Unit at the Institute for
344 Molecular Medicine Finland supported by Biocenter Finland. Johanna Ivaska is thanked for
345 useful comments on the manuscript. Taina Kalevo-Mattila is acknowledged for excellent
346 technical support as well as the entire Turku Bioscience personnel for excellent working
347 environment.
348
349 **Author contributions:** Conception and design: OD, AK, JW. Development of methodology:
350 OD, JM, JW. Experimental work: OD, JM, MT, CS-F, KW. Bioinformatic analysis: LY, MJ.
351 Resources: MO. Writing: OD, JM, TA, JW.
352
353 **Funding:** Project was funded by Jane and Aatos Erkko Foundation (JW), Finnish Cultural
354 Foundation (00160159, OD) and Academy of Finland (TA).
355
356 **Competing interests:** The authors declare no competing interests.
357

358 **Data and materials availability:** All data associated with this study are present in the paper
359 or the Supplementary Materials.
360
361 **Supplementary information**
362 Fig. S1. Interaction of STS derivatives with 300 protein kinases by Chaperone interaction
363 assay.
364 Fig. S2. Immunoblot assessment of PME-1 in T98G cells siRNA kinase screen samples.
365 Fig. S3. Hit validation in heterogeneous GB cell lines.
366 Table S1. Chaperone interaction assay data.
367 Table S2. 28 kinase hit list.
368 Table S3. Custom siRNA kinase library.
369 Table S4. Inhibitor selectivity data.
370 Table S5. A list of siRNAs.
371

372 **References**

373 Berenbaum MC (1989) What is synergy? *Pharmacol Rev* 41: 93-141
374 Brennan CW, Verhaak RG, McKenna A, Campos B, Noushmehr H, Salama SR, Zheng S,
375 Chakravarty D, Sanborn JZ, Berman SH *et al* (2013) The somatic genomic landscape of
376 glioblastoma. *Cell* 155: 462-477
377 Cruz Da Silva E, Mercier MC, Etienne-Selloum N, Dontenwill M, Choulier L (2021) A
378 Systematic Review of Glioblastoma-Targeted Therapies in Phases II, III, IV Clinical Trials.
379 *Cancers (Basel)* 13
380 Dunbar EM, Coats BS, Shroads AL, Langaee T, Lew A, Forder JR, Shuster JJ, Wagner DA,
381 Stacpoole PW (2014) Phase 1 trial of dichloroacetate (DCA) in adults with recurrent
382 malignant brain tumors. *Invest New Drugs* 32: 452-464
383 Gani OA, Engh RA (2010) Protein kinase inhibition of clinically important staurosporine
384 analogues. *Nat Prod Rep* 27: 489-498
385 Gimple RC, Bhargava S, Dixit D, Rich JN (2019) Glioblastoma stem cells: lessons from the
386 tumor hierarchy in a lethal cancer. *Genes Dev* 33: 591-609
387 Guzman C, Bagga M, Kaur A, Westermarck J, Abankwa D (2014) ColonyArea: an ImageJ
388 plugin to automatically quantify colony formation in clonogenic assays. *PloS one* 9: e92444
389 Ianevski A, Giri AK, Aittokallio T (2020) SynergyFinder 2.0: visual analytics of multi-drug
390 combination synergies. *Nucleic acids research* 48: W488-W493
391 Kaley TJ, Panageas KS, Mellinghoff IK, Nolan C, Gavrilovic IT, DeAngelis LM, Abrey LE,
392 Holland EC, Lassman AB (2019) Phase II trial of an AKT inhibitor (perifosine) for recurrent
393 glioblastoma. *J Neurooncol* 144: 403-407
394 Kauko O, Imanishi SY, Kulesskiy E, Yetukuri L, Laajala TD, Sharma M, Pavic K, Aakula A,
395 Rupp C, Jumppanen M *et al* (2020) Phosphoproteome and drug-response effects mediated by
396 the three protein phosphatase 2A inhibitor proteins CIP2A, SET, and PME-1. *Journal of*
397 *Biological Chemistry* 295: 4194-4211
398 Kauko O, O'Connor CM, Kulesskiy E, Sangodkar J, Aakula A, Izadmehr S, Yetukuri L,
399 Yadav B, Padzik A, Laajala TD *et al* (2018) PP2A inhibition is a druggable MEK inhibitor
400 resistance mechanism in KRAS-mutant lung cancer cells. *Science translational medicine* 10
401 Kaur A, Denisova OV, Qiao X, Jumppanen M, Peuhu E, Ahmed SU, Raheem O, Haapasalo
402 H, Eriksson J, Chalmers AJ *et al* (2016) PP2A Inhibitor PME-1 Drives Kinase Inhibitor
403 Resistance in Glioma Cells. *Cancer Res* 76: 7001-7011
404 Klaeger S, Heinzlmeir S, Wilhelm M, Polzer H, Vick B, Koenig PA, Reinecke M, Ruprecht
405 B, Petzoldt S, Meng C *et al* (2017) The target landscape of clinical kinase drugs. *Science* 358
406 Le Joncour V, Filppu P, Hyvonen M, Holopainen M, Turunen SP, Sihto H, Burghardt I,
407 Joensuu H, Tynninen O, Jaaskelainen J *et al* (2019) Vulnerability of invasive glioblastoma
408 cells to lysosomal membrane destabilization. *EMBO Mol Med* 11
409 Lin A, Giuliano CJ, Palladino A, John KM, Abramowicz C, Yuan ML, Sausville EL, Lukow
410 DA, Liu L, Chait AR *et al* (2019) Off-target toxicity is a common mechanism of action of
411 cancer drugs undergoing clinical trials. *Science translational medicine* 11
412 Marcotte R, Brown KR, Suarez F, Sayad A, Karamboulas K, Krzyzanowski PM, Sircoulomb
413 F, Medrano M, Fedyshyn Y, Koh JLY *et al* (2012) Essential gene profiles in breast,
414 pancreatic, and ovarian cancer cells. *Cancer discovery* 2: 172-189
415 Merisaari J, Denisova OV, Doroszko M, Le Joncour V, Johansson P, Leenders WPJ,
416 Kastrinsky DB, Zaware N, Narla G, Laakkonen P *et al* (2020) Monotherapy efficacy of
417 blood-brain barrier permeable small molecule reactivators of protein phosphatase 2A in
418 glioblastoma. *Brain Commun* 2: fcaa002

419 Michelakis ED, Sutendra G, Dromparis P, Webster L, Haromy A, Niven E, Maguire C,
420 Gammer TL, Mackey JR, Fulton D *et al* (2010) Metabolic modulation of glioblastoma with
421 dichloroacetate. *Science translational medicine* 2: 31ra34
422 Montoya S, Soong D, Nguyen N, Affer M, Munamarty SP, Taylor J (2021) Targeted
423 Therapies in Cancer: To Be or Not to Be, Selective. *Biomedicines* 9
424 Mooney J, Bernstock JD, Ilyas A, Ibrahim A, Yamashita D, Markert JM, Nakano I (2019)
425 Current Approaches and Challenges in the Molecular Therapeutic Targeting of Glioblastoma.
426 *World Neurosurg* 129: 90-100
427 Patel AP, Tirosh I, Trombetta JJ, Shalek AK, Gillespie SM, Wakimoto H, Cahill DP, Nahed
428 BV, Curry WT, Martuza RL *et al* (2014) Single-cell RNA-seq highlights intratumoral
429 heterogeneity in primary glioblastoma. *Science* 344: 1396-1401
430 Sangodkar J, Perl A, Tohme R, Kiselar J, Kastrinsky DB, Zaware N, Izadmehr S, Mazhar S,
431 Wiredja DD, O'Connor CM *et al* (2017) Activation of tumor suppressor protein PP2A
432 inhibits KRAS-driven tumor growth. *The Journal of clinical investigation* 127: 2081-2090
433 Shannon P, Markiel A, Ozier O, Baliga NS, Wang JT, Ramage D, Amin N, Schwikowski B,
434 Ideker T (2003) Cytoscape: a software environment for integrated models of biomolecular
435 interaction networks. *Genome Res* 13: 2498-2504
436 Shariati M, Meric-Bernstam F (2019) Targeting AKT for cancer therapy. *Expert Opin*
437 *Investig Drugs* 28: 977-988
438 Stacpoole PW (2017) Therapeutic Targeting of the Pyruvate Dehydrogenase
439 Complex/Pyruvate Dehydrogenase Kinase (PDC/PDK) Axis in Cancer. *J Natl Cancer Inst*
440 109
441 Szklarczyk D, Gable AL, Nastou KC, Lyon D, Kirsch R, Pyysalo S, Doncheva NT, Legeay
442 M, Fang T, Bork P *et al* (2021) The STRING database in 2021: customizable protein-protein
443 networks, and functional characterization of user-uploaded gene/measurement sets. *Nucleic*
444 *acids research* 49: D605-D612
445 Taipale M (2018) Quantitative Profiling of Chaperone/Client Interactions with LUMIER
446 Assay. *Methods Mol Biol* 1709: 47-58
447 Taipale M, Krykbaeva I, Whitesell L, Santagata S, Zhang J, Liu Q, Gray NS, Lindquist S
448 (2013) Chaperones as thermodynamic sensors of drug-target interactions reveal kinase
449 inhibitor specificities in living cells. *Nature biotechnology* 31: 630-637
450 Tang J, Tanoli ZU, Ravikumar B, Alam Z, Rebane A, Vaha-Koskela M, Peddinti G, van
451 Adrichem AJ, Wakkinen J, Jaiswal A *et al* (2018) Drug Target Commons: A Community
452 Effort to Build a Consensus Knowledge Base for Drug-Target Interactions. *Cell Chem Biol*
453 25: 224-229 e222
454 Vervoort SJ, Welsh SA, Devlin JR, Barbieri E, Knight DA, Offley S, Bjelosevic S,
455 Costacurta M, Todorovski I, Kearney CJ *et al* (2021) The PP2A-Integrator-CDK9 axis fine-
456 tunes transcription and can be targeted therapeutically in cancer. *Cell* 184: 3143-3162 e3132
457 Wen PY, Touat M, Alexander BM, Mellinghoff IK, Ramkissoon S, McCluskey CS, Pelton
458 K, Haidar S, Basu SS, Gaffey SC *et al* (2019) Buparlisib in Patients With Recurrent
459 Glioblastoma Harboring Phosphatidylinositol 3-Kinase Pathway Activation: An Open-Label,
460 Multicenter, Multi-Arm, Phase II Trial. *Journal of clinical oncology : official journal of the*
461 *American Society of Clinical Oncology* 37: 741-750
462 Westermarck J (2018) Targeted therapies don't work for a reason; the neglected tumor
463 suppressor phosphatase PP2A strikes back. *The FEBS journal* 285: 4139-4145

464